Biochemical and Biophysical Research Communications **268,** 14–19 (2000)
doi:10.1006/bbrc.1999.2069, available online at http://www.idealibrary.com on IDEAL®

Acetylation at the N-Terminus of Actin Strengthens Weak Interaction between Actin and Myosin

Akinobu Abe, Kimiko Saeki, Takuo Yasunaga, and Takeyuki Wakabayashi[1]
Department of Physics, School of Science, University of Tokyo, Hongo 7-3-1, Bunkyo-ku, Tokyo 113-0033, Japan

Received December 24, 1999

The N-terminus of all actins so far studied is acetylated. Although the pathways of acetylation have been well studied, its functional importance has been unclear. A negative charge cluster in the actin N-terminal region is shown to be important for the function of actomyosin. Acetylation at the N-terminus removes a positive charge and increases the amount of net negative charges in the N-terminal region. This may augment the role of the negative charge cluster. To examine this possibility, actin with a nonacetylated N-terminus (nonacetylated actin) was produced. The nonacetylated actin polymerized and depolymerized normally. In actin-activated heavy meromyosin ATPase assays, the nonacetylated actin showed higher K_{app} without significantly changing V_{max}, compared with those of wild-type actin. This is in contrast to the effect of the N-terminal negative charge cluster, which increases V_{max} without changing K_{app}. These results indicate that the acetylation at the N-terminus of actin strengthens weak actomyosin interaction.

Key Words: **actin N-terminal acetylation; actin-activated myosin ATPase; actomyosin interaction; histidine-tagged actin.**

The N-terminus of all actins so far studied is acetylated as the result of actin N-terminal processing, whose pathways have been well studied. Actins are divided into two classes on the basis of the nucleotide sequences encoding their N-termini. Each class has different pathway of processing. For class I actins, such as *Dictyostelium* actin and β-actin, the N-terminal sequence is Met-Asp(Glu)- on their genes, whereas the sequence is *N*-acetyl-Asp(Glu)- on mature actin. The methionyl residue at its N-terminus is acetylated after the translation and removed as *N*-acetylmethionine. Then, the newly generated amino group is acetylated (1). The genes for class II actins, such as skeletal muscle actin and *Drosophila* actin, usually encode Met-Cys-Asp(Glu)- for their N-termini, whereas the mature class II actins have *N*-acetyl-Asp(Glu)- sequences. During the translation, unmodified methionine is removed from the N-terminus and the cysteinyl residue that newly becomes the N-terminus is acetylated. After the translation, the *N*-acetylcysteine is removed and the N-terminal acetylation occurs again (2).

The factors that promote the N-terminal processing of actin should be specific to actin for the following reasons. (I) Usually, N-terminal acetylation occurs in the case that the amino acid residue at the N-terminus is alanine, threonine, serine, glycine, or methionine (3). However, actin has a negatively charged residue (Asp or Glu) at its acetylated N-terminus. (II) In general, methionine is removed from the N-terminus of a protein if the next residue is small and uncharged (3). However, the N-terminal methionine of class I actin is removed even if the side chain of the second residue has a negative charge. (III) *N*-acetylaminopeptidase that is specific to actin has been isolated from rat liver (4). These facts suggest that the N-terminal acetylation of actin through the processing should be important for the function of actin. However, the functional importance has been unclear.

On the other hand, the N-terminal sequence 1–4 of actins is rich in acidic amino acid residues and forms a negative charge cluster. The sequences are, for example, Acetyl-Asp-Glu-Asp-Glu- for rabbit skeletal muscle actin and Acetyl-Asp-Gly-Glu-Asp- for *Dictyostelium discoideum* actin. The previous studies have revealed that the negative charge cluster in actin N-terminal amino acid residues 1–4 are important for the function of actomyosin (5–13). It increases V_{max} of actin-activated ATPase of myosin without changing K_{app} appreciably. N-terminal acetylation may contribute to such an effect, because it increases the number of net negative charges in the N-terminal region of actin by removing a positive charge from the N-terminal α-amino group.

Abbreviations used: *p*-APMSF, *p*-amidinophenylmethanesulfonyl fluoride; HMM, heavy meromyosin; Ni–NTA, nickel–nitrilotriacetate; PAGE, polyacrylamide gel electrophoresis; S1, myosin subfragment-1; SDS, sodium dodecyl sulfate.

[1] To whom correspondence should be addressed. Fax: +81-3-5841-4157. E-mail: wakabayashi@phys.s.u-tokyo.ac.jp.

0006-291X/00 $35.00

To examine this possibility, we have produced actin with nonacetylated N-terminus (nonacetylated actin) and compared its biochemical properties with those of wild-type actin. To prepare the nonacetylated actin, *Dictyostelium* actin to which 10-histidine tag and a factor Xa recognition sequence (-Ile-Glu-Gly-Arg-) were genetically added at its N-terminus was isolated and digested with factor Xa. Having the unblocked N-terminus, the obtained actin was the same as the non-acetylated actin. The nonacetylated actin formed normal filaments, bound myosin subfragment-1 (S1) strongly, and activated heavy meromyosin (HMM) ATPase. Compared with wild-type actin, the nonacetylated actin showed higher K_{app} without significantly changing V_{max}. Thus, the effect of the N-terminal acetylation of actin on actomyosin ATPase cycle cannot be explained by its effect on the charges of the N-terminal region. The effect of the acetylation at the N-terminus of actin is different: it facilitates the weak interaction between actin and myosin in actomyosin ATPase cycle.

Some of the present results have been reported in a preliminary form (14).

MATERIALS AND METHODS

Materials. Ni–NTA agarose was purchased from Qiagen. Factor Xa was purchased from New England Biolabs. An anti-actin polyclonal antibody A2066 and *p*-amidinophenylmethanesulfonyl fluoride (*p*-APMSF) were purchased from Sigma. NanoVan was purchased from Nanoprobes.

Plasmid construction. The coding sequence of both 10-histidine tag and factor Xa recognition sequence (-Ile-Glu-Gly-Arg-) was inserted into the actin 15 gene (15) immediately after the start codon by oligonucleotide-directed mutagenesis (16). This 10-histidine-tagged actin with factor Xa recognition sequence at its N-terminus was designated as H_{10}Xa-actin.

A transformation vector was constructed by inserting the mutant actin 15 gene into an extrachromosomal vector pBIG (17) as described (18).

Transformation of Dictyostelium cells. The transformation vector was introduced into *Dictyostelium* cells by electroporation (19). Transformed cells were selected by culturing them in the presence of G418 (neomycin analogue) as described (6). The expression of H_{10}Xa-actin was confirmed by SDS–PAGE because the addition of 10-histidine tag and factor Xa recognition sequence to the N-terminus of actin increased the molecular weight of actin.

Preparation of proteins. All procedures were carried out on ice or at 4°C unless otherwise stated.

When the number of *Dictyostelium* cells expressing H_{10}Xa-actin reached 1×10^{10} in 4-L culture (2.5×10^6/mL), the cells were harvested by centrifugation. The cells were then washed twice with G buffer (20 mM imidazole-acetate, pH 7.4, 0.2 mM calcium acetate, 0.5 mM ATP, and 1 mM β-mercaptoethanol) and finally suspended in G buffer containing 1 mM phenylmethanesulfonyl fluoride, 0.1 mg/ml leupeptin, 0.02 mg/ml chymostatin, and 0.02 mg/ml pepstatin. The suspended cells were sonicated for six 10-s periods and centrifuged at 25,000*g* for 30 min. The supernatant was stirred for 2 h with Ni–NTA agarose equilibrated with G buffer. The resin was washed with G buffer five times to remove unbound proteins, including wild-type actin. H_{10}Xa-actin was eluted by suspending the resin in 200 mM imidazole–acetate, pH 7.4, 0.2 mM calcium acetate, 0.5 mM ATP, and 1 mM β-mercaptoethanol. Then, H_{10}Xa-actin was mixed with factor Xa at a ratio of 1:20 (w/w) and was dialyzed against G buffer at room temperature for 2 days. The reaction was stopped by adding a 10,000-fold molar excess of *p*-APMSF over factor Xa. Fragments containing 10-histidine tag and factor Xa recognition sequence, and undigested H_{10}Xa-actin were removed by stirring the solution for 2 h with Ni–NTA agarose equilibrated with G buffer. The supernatant was collected by centrifugation and dialyzed against 20 mM imidazole–HCl, pH 7.0, 100 mM KCl, 5 mM $MgCl_2$, 0.5 mM ATP, and 1 mM β-mercaptoethanol overnight. The resulting F-actin was ultracentrifuged at 541,000*g* for 30 min in a Beckman TL-100 ultracentrifuge. The F-actin pellet was resuspended in 10 mM imidazole–HCl, pH 7.0, 0.2 mM $MgCl_2$, 0.5 mM ATP, and 1 mM β-mercaptoethanol, and dialyzed against the same solvent overnight. The resulting solution was finally cleared by ultracentrifugation at 436,000*g* for 10 min in a Beckman TL-100 ultracentrifuge. The supernatant contained the homogeneous non-acetylated actin. The yield of the purified actin was 300 μg from a 1-L culture.

Wild-type actin was prepared from Ax2 cells as described (6). Rabbit skeletal actin was prepared from rabbit skeletal muscle acetone powder (20). Myosin was prepared from rabbit skeletal muscle (21). Heavy meromyosin (HMM) and myosin subfragment-1 (S1) was obtained by digesting myosin with chymotrypsin following the procedure described previously (22, 23).

ATPase measurements. ATPase activities were measured as described (6) in 2.5 mM KCl, 10 mM imidazole–HCl, pH 7.0, 4 mM $MgCl_2$, 1 mM ATP, 5 μg/ml phalloidin, 0.03 mg/ml HMM, and 0–50 μM actin at 25°C. Liberated phosphate was measured by the malachite green method (24).

Electron microscopy. Polymerized actin for electron microscopy was formed in 10 mM imidazole–HCl, pH 7.0, 50 mM KCl, 2 mM $MgCl_2$, 0.5 mM ATP, and 1 mM DTT at 25°C for 2 h. The polymerized actin was mounted on carbon film and negatively stained with NanoVan, pH 8.0. Electron micrographs were taken at an instrumental magnification of 30,000 on Kodak SO163 film with Hitachi HF2000 electron microscope operated at 200 kV. The electron dose was about 15 $e^-/Å^2$.

Other procedures. SDS–PAGE was done on 10% (w/v) polyacrylamide slab gels (25), and gels were stained with Coomassie brilliant blue. Two-dimensional electrophoresis was carried out by the method of O'Farrel (26) and Mikawa *et al.* (27). The first dimension (isoelectric focusing) was performed in the presence of 9 M urea. The second dimension was SDS–PAGE. Gels were stained with Coomassie brilliant blue.

Protein concentration of rabbit skeletal actin, HMM, and S1 was measured by determining absorbance at 280 nm with the extinction coefficient as 11.1 cm^{-1} (1%) (28), 6.0 cm^{-1} (1%), and 7.5 cm^{-1} (1%) (29), respectively. Protein concentration of wild-type and the non-acetylated actin was measured by the Bradford method (30) according to Read and Northcote (31) with rabbit skeletal actin as standard.

Binding of myosin subfragment-1 (S1) to non-acetylated actin filaments in the absence of ATP was examined by cosedimentation experiments. Mixture composed of 50 mM KCl, 10 mM imidazole–HCl, pH 7.0, 2 mM $MgCl_2$, and 1 mM DTT, 0.87 μM S1 were ultracentrifuged in the presence or absence of 7.5 μM nonacetylated actin at 4°C for 10 min in a Beckman TL-100 ultracentrifuge. The resulting pellets were resuspended in the same buffer in volumes equal to those of the supernatants, and then samples of both supernatants and resuspended pellets were subjected to SDS–PAGE. The gel was stained with Coomassie brilliant blue.

RESULTS

Preparation of Nonacetylated Actin

A new polypeptide band appeared at the position corresponding to slightly larger molecular weight than that of wild-type actin in an SDS–PAGE pattern of the

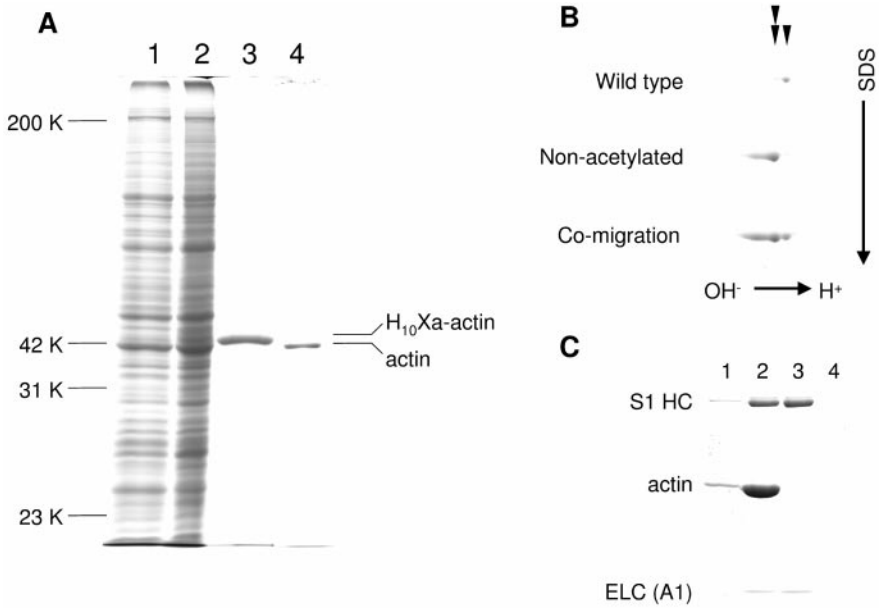

FIG. 1. Preparation of actin with nonacetylated N-terminus (nonacetylated actin). (A) An SDS–PAGE pattern showing each purification step of the nonacetylated actin. Lane 1, whole lysate of Ax2 cells; lane 2, whole lysate of cells expressing H_{10}Xa-actin (actin with 10-histidine tag and factor Xa recognition sequence at its N-terminus); lane 3, H_{10}Xa-actin; lane 4, nonacetylated actin. Proteins were separated on 10% (w/v) SDS–polyacrylamide gel and stained with Coomassie brilliant blue. (B) Two-dimensional gel electrophoretic patterns of purified wild-type or nonacetylated actin, or the mixture of them. Single and double arrowheads indicate wild-type actin and the nonacetylated actin, respectively. (C) Cosedimentation of myosin subfragment-1 (S1) with nonacetylated actin filaments in the absence of ATP. Cosedimentation experiments were performed in 50 mM KCl, 10 mM imidazole–HCl, pH 7.0, 2 mM $MgCl_2$, 1 mM DTT, 0.87 μM S1 at 25°C in the presence (lanes 1 and 2) or absence (lanes 3 and 4) of 7.5 μM nonacetylated actin. The supernatants (lanes 1 and 3) and precipitates (lanes 2 and 4) were loaded onto 10% (w/v) SDS–polyacrylamide gel and stained with Coomassie brilliant blue. HC, heavy chain; ELC, essential light chain.

whole lysate prepared from cells transformed with a vector containing H_{10}Xa-actin gene (Fig. 1A, lanes 1 and 2). We concluded that the polypeptide was H_{10}Xa-actin, because the polypeptide reacted with an antibody raised against the C-terminal amino acid residues 365–375 of actin (data not shown), and because it attached to and detached from Ni–NTA resin, depending on the concentration of imidazole.

H_{10}Xa-actin was completely separated from wild-type actin with Ni–NTA resin (Fig. 1A, lane 3). The elution of H_{10}Xa-actin from Ni–NTA resin was usually carried out keeping its concentration as low as 0.1–0.3 mg/ml, because H_{10}Xa-actin aggregated at higher concentration when the concentration of imidazole was 200 mM.

Because the proteolytic activity of factor Xa was inhibited by 200 mM imidazole, H_{10}Xa-actin was digested at low imidazole concentration (20 mM). At this concentration of imidazole, H_{10}Xa-actin was soluble up to about 0.1 mg/ml. Hence, the concentration of H_{10}Xa-actin was kept 0.1 mg/ml or less during the digestion. Under these conditions, about half amount of H_{10}Xa-actin was digested with factor Xa to generate the nonacetylated actin. The undigested H_{10}Xa-actin, and fragments containing 10-histidine tag and factor Xa recognition sequence were removed with Ni–NTA resin. Finally, a polymerization–depolymerization cycle was done to separate the non-acetylated actin from factor Xa (Fig. 1A, lane 4).

The nonacetylated actin did not aggregate any more even under the conditions mentioned above. On the other hand, a similar tendency to aggregate was observed for actin with 10-histidine tag and *without* factor Xa recognition sequence at its N-terminus. Therefore, the aggregation of H_{10}Xa-actin was probably due to the existence of 10-histidine tag at its N-terminus.

Two-dimensional electrophoretic patterns of purified wild-type or nonacetylated actin, or the mixture of them revealed that the nonacetylated actin was more basic than wild-type actin, as expected (Fig. 1B).

The nonacetylated actin polymerized and depolymerized normally. Figure 2 shows an electron micrograph of the nonacetylated actin filaments. The crossover periods were about 36 nm, indicating that the nonacetylated actin formed normal filaments.

Myosin subfragment-1 cosedimentated with nonacetylated actin filaments in the absence of ATP (Fig. 1C). This means that the nonacetylated actin forms rigor complex with myosin.

Actin-Activated ATPase Activity of HMM

Actin-activated ATPase activities of HMM were measured in the presence of various amounts of wild-

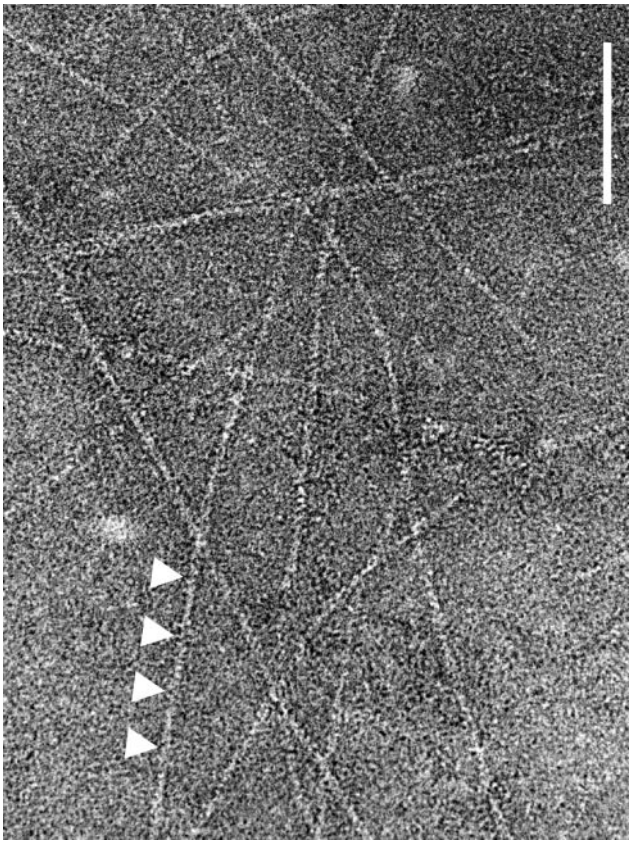

FIG. 2. An electron micrograph of the nonacetylated actin filaments. The nonacetylated actin filaments (0.1 mg/ml) were negatively stained with NanoVan, pH 8.0. Arrowheads indicate crossover points of actin helix with an interval of 36 nm. Bar, 100 nm.

type or the nonacetylated actin filaments. Figure 3 shows the results as an Eadie–Hofstee plot. The V_{max} and K_{app} values were obtained from this plot.

V_{max} is the maximum turnover rate of acto-HMM ATPase at infinite actin concentration and means the maximum extent of the activation of myosin ATPase by actin. The intercept on the ordinate of Fig. 3 corresponds to V_{max}. The V_{max} value for wild-type actin was $13.5 \pm 1.0\ s^{-1}$, and that for the nonacetylated actin was $17.4 \pm 2.0\ s^{-1}$. Namely, the V_{max} values showed that the difference between the two actins is not so significant.

K_{app} is the concentration of actin that gives the half rate of V_{max} of acto-HMM ATPase. This means that $1/K_{app}$ represents the apparent affinity between actin and HMM in the presence of ATP, that is, the extent of weak interaction between the two proteins. The slope of Fig. 3 corresponds to $-K_{app}$. The K_{app} value for wild-type actin was $25.5 \pm 3.0\ \mu M$, and that for the nonacetylated actin was $91.9 \pm 12.8\ \mu M$. Namely, the K_{app} value for the nonacetylated actin was 3.6 times larger than that for wild-type actin, indicating that the acetylation at the N-terminus of actin strengthens weak interaction between actin and myosin during actomyosin ATPase cycle.

DISCUSSION

We have found that the N-terminal acetylation of actin decreases K_{app} (dissociation constant) of acto-HMM ATPase and keeps V_{max} almost unaffected. Considering these results, we compare the effect of the acetylation with that of the N-terminal negative charge cluster of actin.

Preparation of Nonacetylated Actin

We have succeeded in expressing and purifying N-terminal 10-histidine-tagged *Dictyostelium* actin with factor Xa recognition sequence (H_{10}Xa-actin). Our affinity-chromatographic method has realized separation of mutant actins not separable from wild-type actin by the previous method utilizing anion exchange chromatography (6, 12, 32).

Unlike the previous histidine-tagged actin (33), H_{10}Xa-actin has a cleavable histidine tag. Because the nonacetylated actin generated from H_{10}Xa-actin differs from wild-type actin only in its nonacetylated N-terminus, it has enabled unambiguous elucidation of the functional importance of the acetylation, in contrast to previous nonacetylated actins (10, 34–37).

Actin-Activated ATPase Activity of HMM

V_{max} of acto-HMM ATPase was almost unchanged whether the N-terminus was acetylated or not, indicating that the effect of the acetylation on the extent of

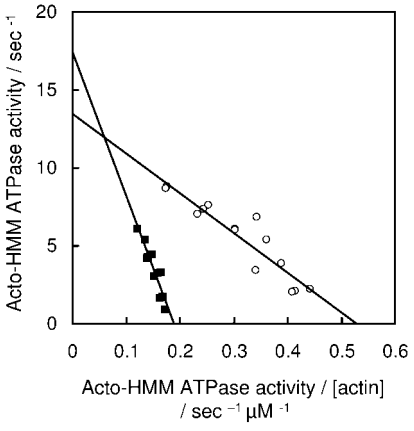

FIG. 3. Eadie–Hofstee plot of the actin-activated ATPase of HMM for wild-type (circles) or the nonacetylated actin (squares). The ATPase activity was measured in 2.5 mM KCl, 10 mM imidazole–HCl, pH 7.0, 4 mM $MgCl_2$, 1 mM ATP, 5 μg/ml phalloidin, 0.03 mg/ml HMM, and 0–50 μM actin at 25°C. The intercept on the ordinate, and the slope represent V_{max} and $-K_{app}$, respectively. The V_{max} value for wild-type actin was $13.5 \pm 1.0\ s^{-1}$, and that for the non-acetylated actin was $17.4 \pm 2.0\ s^{-1}$. The K_{app} value for wild-type actin was $25.5 \pm 3.0\ \mu M$, and that for the nonacetylated actin was $91.9 \pm 12.8\ \mu M$, indicating that the acetylation at the N-terminus of actin strengthens weak interaction between actin and myosin in the presence of ATP.

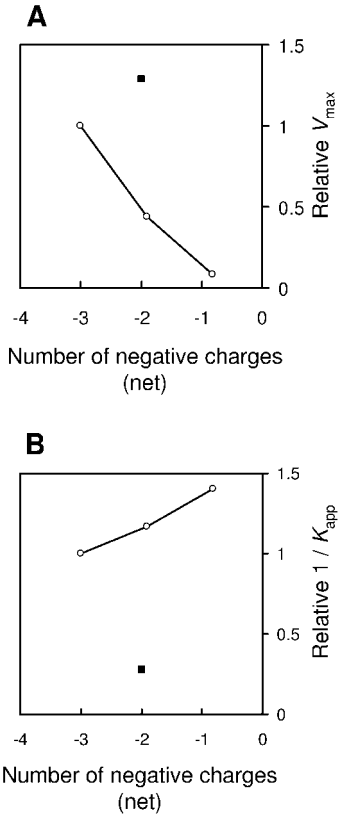

FIG. 4. Comparison of kinetic parameters of acto-HMM ATPase reaction between the nonacetylated actin (squares) and *Dictyostelium* wild-type or N-terminal mutant actins (circles). V_{max} (A) and $1/K_{app}$ (B) normalized with the values for wild-type actin as unit were plotted against the number of net negative charges in actin N-terminal residues 1–4. The mutant actins plotted were D1H and D1H/D4H (6). The number of net charges at pH 7.0 was calculated as described (38) to obtain −3.0 for wild type, −1.9 for D1H, −0.82 for D1H/D4H, and −2.0 for the nonacetylated actin.

activation of myosin ATPase was small. On the other hand, the nonacetylated actin showed 3.6 times higher K_{app} than that of wild-type actin. This means that $1/K_{app}$, representing the apparent affinity between actin and HMM in the presence of ATP, is smaller if the N-terminus is not acetylated, and therefore indicates that the N-terminal acetylation of actin strengthens weak actomyosin interaction.

Previous studies have revealed that the number of negative charges in actin N-terminal sequence 1–4 correlates with V_{max} and K_{app} (6, 7, 11–13). Figure 4A shows that V_{max} increases dramatically as the number of negative charges rises from about 1 to 3. On the other hand, as seen from Fig. 4B, $1/K_{app}$ does not show such large change. Although the charges in the sequence 1–4 of the non-acetylated actin was −2, it had almost the same V_{max} as that of wild-type actin, which had 3 negative charges in the same region (Fig. 4A). This means that the activation of myosin ATPase by the nonacetylated actin is higher than expected from the number of the negative charges. On the other hand, the nonacetylated actin showed much lower $1/K_{app}$ (Fig. 4B). Namely, weak interaction of the nonacetylated actin with myosin is much lower than expected. These results suggest that the effect of the acetylation at the N-terminus of actin on actomyosin interaction is different from that of the N-terminal negative charge cluster.

The hydrophobicity of the nonacetylated N-terminus should be smaller than that of the acetylated one, because the N-terminal á-amino group has a positive charge and the hydrophobic acetyl group is removed. This decrease in hydrophobicity may be related to the unexpected decrease in the weak interaction. In the weakly bound complex, the positive charge may be screened, possibly, by myosin residues so that the N-terminal three negative charges can activate myosin ATPase normally. This may result in the almost unchanged V_{max}.

In conclusion, the N-terminal acetylation of actin increases weak actomyosin interaction about 3.6 times without significantly affecting the maximum extent of actin-activation of myosin ATPase. These results are specific to the N-terminal acetylation and cannot be accounted for by changes of negative charges in the N-terminal region.

ACKNOWLEDGMENTS

pBIG vector was kindly provided by Dr. Spudich (Stanford University), Dr. Patterson (University of Arizona), and Dr. Uyeda (National Institute for Advanced Interdisciplinary Research, Tsukuba, Japan). We thank Dr. Sutoh (University of Tokyo) for fruitful discussions. This work was supported by a Grant-in-Aid for General Scientific Research and Specially Promoted Scientific Research from the Ministry of Education, Science, Sports, and Culture of Japan, an HFSP grant, a grant for “Biodesign Research Program” from the Institute of Physical Chemical Research (RIKEN), and a grant from the Mitsubishi Foundation to T.W.

REFERENCES

1. Rubenstein, P. A., Redman, K. L., Solomon, L. R., and Martin, D. J. (1987) *Methods Cell Biol.* **28,** 231–243.
2. Martin, D. J., and Rubenstein, P. A. (1987) *J. Biol. Chem.* **262,** 6350–6356.
3. Bradshaw, R. A., Brickey, W. W., and Walker, K. W. (1998) *Trends Biochem. Sci.* **23,** 263–267.
4. Sheff, D. R., and Rubenstein, P. A. (1992) *J. Biol. Chem.* **267,** 20217–20224.
5. Sutoh, K. (1982) *Biochemistry* **21,** 3654–3661.
6. Sutoh, K., Ando, M., Sutoh, K., and Toyoshima, Y. Y. (1991) *Proc. Natl. Acad. Sci. USA* **88,** 7711–7714.
7. Sutoh, K. (1993) *Adv. Exp. Med. Biol.* **332,** 241–244.
8. Aspenström, P., and Karlsson, R. (1991) *Eur. J. Biochem.* **200,** 35–41.
9. Aspenström, P., Lindberg, U., and Karlsson, R. (1992) *FEBS Lett.* **303,** 59–63.
10. Cook, R. K., Blake, W. T., and Rubenstein, P. A. (1992) *J. Biol. Chem.* **267,** 9430–9436.

11. Cook, R. K., Root, D., Miller, C., Reisler, E., and Rubenstein, P. A. (1993) *J. Biol. Chem.* **268,** 2410–2415.
12. Saeki, K., Sutoh, K., and Wakabayashi, T. (1996) *Biochemistry* **35,** 14465–14472.
13. Miller, C. J., Wong, W. W., Bobkova, E., Rubenstein, P. A., and Reisler, E. (1996) *Biochemistry* **35,** 16557–16565.
14. Abe, A., Saeki, K., Yasunaga, T., Sutoh, K., and Wakabayashi, T. (1999) *Biophys. J.* **76,** A39.
15. Knecht, D. A., Cohen, S. M., Loomis, W. F., and Lodish, H. F. (1986) *Mol. Cell. Biol.* **6,** 3973–3983.
16. Kunkel, T. A. (1985) *Proc. Natl. Acad. Sci. USA* **82,** 488–492.
17. Ruppel, K. M., Uyeda, T. Q. P., and Spudich, J. A. (1994) *J. Biol. Chem.* **269,** 18773–18780.
18. Sambrook, J., Fritsch, E. F., and Maniatis, T. (1989) Molecular Cloning: A Laboratory Manual, 2nd ed., Cold Spring Harbor Laboratory Press, Cold Spring Harbor, NY.
19. Howard, P. K., Ahern, K. G., and Firtel, R. A. (1988) *Nucleic Acids Res.* **16,** 2613–2623.
20. Spudich, J. A., and Watt, S. (1971) *J. Biol. Chem.* **246,** 4866–4871.
21. Szent-Györgyi, A. (1951) Chemistry of Muscle Contraction, 2nd ed., Academic Press, New York.
22. Weeds, A. G., and Taylor, R. S. (1975) *Nature* **257,** 54–56.
23. Okamoto, Y., and Sekine, T. *J. Biochem.* **98,** 1143–1145.
24. Kodama, T., Fukui, K., and Kometani, K. (1986) *J. Biochem.* **99,** 1465–1472.
25. Laemmli, U. K. (1970) *Nature* **227,** 680–685.
26. O'Farrell, P. H. (1975) *J. Biol. Chem.* **250,** 4007–4021.
27. Mikawa, T., Takeda, S., Shimizu, T., and Kitaura, T. (1981) *J. Biochem.* **89,** 1951–1962.
28. Houk, T. W., Jr., and Ue, K. (1974) *Anal. Biochem.* **62,** 66–74.
29. Margossian, S. S., and Lowey, S. (1982) *Methods Enzymol.* **85,** 55–71.
30. Bradford, M. M. (1976) *Anal. Biochem.* **72,** 248–254.
31. Read, S. M., and Northcote, D. H. (1981) *Anal. Biochem.* **116,** 53–64.
32. Johara, M., Toyoshima, Y. Y., Ishijima, A., Kojima, H., Yanagida, T., and Sutoh, K. (1993) *Proc. Natl. Acad. Sci. USA* **90,** 2127–2131.
33. Buzan, J., Du, J., Karpova, T., and Frieden, C. (1999) *Proc. Natl. Acad. Sci. USA.* **96,** 2823–2827.
34. Solomon, T. L., Solomon, L. R., Gay, L. S., and Rubenstein, P. A. (1988) *J. Biol. Chem.* **263,** 19662–19669.
35. Cook, R. K., Sheff, D. R., and Rubenstein, P. A. (1991) *J. Biol. Chem.* **266,** 16825–16833.
36. Sheff, D. R., and Rubenstein, P. A. (1992) *J. Biol. Chem.* **267,** 2671–2678.
37. Hennessey, E. S., Drummond, D. R., and Sparrow, J. C. (1991) *Eur. J. Biochem.* **197,** 345–352.
38. Skoog, B., and Wichman, A. (1986) *Trends Anal. Chem.* **5,** 82–83.